JOURNAL OF GEOPHYSICAL RESEARCH, VOL. 113, A01206, doi:10.1029/2007JA012601, 2008

Jupiter's changing auroral location

Denis Grodent,[1] Jean-Claude Gérard,[1] Aikaterini Radioti,[1] Bertrand Bonfond,[1] and Adem Saglam[1]

Received 20 June 2007; revised 31 August 2007; accepted 9 October 2007; published 22 January 2008.

[1] We examine the case of significant latitudinal shifts of the Jovian northern auroral emissions appearing in a data set spanning nine years of observations with the Hubble Space Telescope in the far ultraviolet. The extended data set makes it possible to compare the location of the main auroral emission with similar viewing geometries and satellite positions. The main auroral emission is assumed to originate from beyond the orbit of Ganymede (15 Jovian radii). At these distances, near corotation enforcement and transfer of momentum from Jupiter to the magnetospheric plasma is ensured by means of field aligned currents. The field aligned currents away from Jupiter are carried by downward energetic electrons loosing their energy to the polar atmosphere and giving rise to the main auroral emission. Analysis of the polar projected images shows that the latitudinal location of the main emission has changed by up to 3° over long periods of time. It also shows that the footprint of Ganymede follows a similar trend. We have used the VIP4 magnetic field model to map the emission down to the equatorial plane. This mapping suggests that internal variations of the current sheet parameters might be used as an alternative or complementary explanation to the changing solar wind conditions at Jupiter to explain the observed shift of auroral latitudes.

Citation: Grodent, D., J.-C. Gérard, A. Radioti, B. Bonfond, and A. Saglam (2008), Jupiter's changing auroral location, *J. Geophys. Res.*, *113*, A01206, doi:10.1029/2007JA012601.

1. Introduction

[2] Hubble Space Telescope (HST) images have shown that Jupiter's aurora exhibits three distinct components based on their locations, the physical regions and processes from which they originate, and their independent variations with time [*Clarke et al.*, 1998, 2002]. These three components can be summarized as the satellite footprint emissions, the main auroral oval, and the polar emissions [*Grodent et al.*, 2003a, 2003b]. The main Jovian auroral oval is likely connected with the magnetosphere-ionosphere coupling current system associated with the breakdown of rigid corotation in the middle magnetosphere region [*Bunce and Cowley*, 2001a; *Hill*, 2001; *Southwood and Kivelson*, 2001]. It may thus be interpreted as the ionospheric footprint of the upward Birkeland current that enforces partial corotation of magnetospheric plasma moving outward from the Io plasma torus to the outer magnetosphere. The equatorial source of these outward field-aligned currents is broadly distributed within the middle magnetosphere current sheet, between inner distances of ~20 Jovian radii (R_J) and outer distances of several tens of R_J, bounded by the radial extent of the current sheet. Accordingly, the main auroral emission connects emission features that may very well map to different regions of the magnetosphere and it should not be assumed to be a fixed radial distance footprint.

[3] The concept of main auroral oval is somewhat misleading because it suggests a static narrow ring of emission closing around the magnetic pole. It also suggests that the same magnetospheric mechanism produces the emission everywhere around Jupiter. However, individual ultraviolet auroral images of Jupiter's North Pole show that the narrow structured portion of the main oval represents only a fraction of the main oval and is usually restricted to the dawn to noon sector. The rest of the emission forms unstructured features in the noon to dusk region. Consequently, it is not always possible to define a closed auroral contour around the pole. Even so, it is certainly not shaped like an oval [e.g., *Grodent et al.*, 2003a]. For these reasons we prefer to call this emission, which is believed to be mostly related to the corotation breakdown enforcement mechanism, the main emission (ME) instead of main oval emission.

[4] *Grodent et al.* [2003a] showed that the general shape of the ME remains roughly constant, even over time periods spanning several years. They took advantage of the relative stability of the ME to define reference ovals, better named "contours", to provide the average or the most likely location of auroral emissions. These reference contours were used to estimate the actual stability of the ME. *Grodent et al.* [2003a] noticed a local time contraction of the ME in a set of HST images obtained during the period of the Cassini flyby, in December 2000 and January 2001. This poleward shift is on the order of 2°, it occurs between

[1]Laboratory for Planetary and Atmospheric Physics, Université de Liège, Belgium.

0148-0227/08/2007JA012601$09.00

images obtained with a central meridian longitude (CML) increasing from 115 to 255°. A secondary contraction, of the same order of magnitude and affecting all local times, was found to take place on a longer timescale. It appeared that the ME was smaller than the reference contour on 14 December 2000, 13 January 2001, and 20 January 2001, with the most pronounced effect occurring on 13 January 2001. These morphological changes are of the same order as the mapping accuracy of the emission and should be considered with caution. They were tentatively attributed to the expansion phase of the magnetosphere that followed the compression induced by the arrival of an interplanetary shock or to a time of increased solar wind dynamic pressure. More recently, *Nichols et al.* [2007] compared the 2000–2001 HST data set with the in situ field and particles observations obtained simultaneously with the Cassini spacecraft. They concluded that, within the timing uncertainties induced by the propagation of the solar wind conditions from the spacecraft to Jupiter, the brightened images (including the extreme case obtained on 13 January 2001) corresponded to an interval of enhanced solar wind conditions and consequent magnetospheric dynamics, in which the magnetosphere underwent a modest compression followed by an extended major expansion. However, uncertainties on the modeling of the solar wind parameters did not permit them to conclude whether the brightenings occurred during the expansion or the contraction of the magnetosphere. The latter case would contradict the theoretical picture presented by *Southwood and Kivelson* [2001] and *Cowley and Bunce* [2001, 2003a, 2003b] in which auroral brightening is associated with magnetospheric expansion. *Cowley and Bunce* [2003a, 2003b] also showed that transient super-corotation could be excited by a sudden compression of the magnetosphere from ~70 to ~45 R_J. However, these studies only modeled the response of the middle magnetosphere, so that the issue of the formation of a new poleward oval resulting from a reversal in the sense of the magnetosphere-ionosphere coupling current system could not be quantitatively investigated. In a recent modeling effort, *Cowley et al.* [2007] included the response of the outer magnetosphere and of a region of open field lines mapping to the tail. They suggested that magnetospheric reconfigurations, compressions or expansions, by sudden changes in the dynamic pressure of the solar wind are a relatively short timescale process taking place over a few Jovian rotations. They are shown to have large dynamical effects on the auroral brightness distribution and, in the case of super-rotation following strong compression of the magnetosphere, to form a two-ring auroral system, the poleward one (several degrees) corresponding to the open-closed field line boundary, the other to the middle magnetosphere.

[5] In the present study, we examine the case of large poleward/equatorward shifts of the ME showing up in a much more extended data set spanning nine years of HST observations. These shifts are possibly similar to the secondary long term (days) contraction of the ME in the winter 2000–2001 data set discussed by *Grodent et al.* [2003a]. The extended data set makes it possible to use the auroral footprint of Ganymede as a landmark for the location of the ME which is assumed to originate from beyond the orbit of Ganymede (15 R_J). In addition, by comparing data sets spanning several months or years, we increase the chances to observe long term auroral variations, including these resulting from possible current sheet variations, which otherwise could not be detected. It should be noted, however, that the poor sampling rate of the HST data set that has been considered in this study does not allow us to conclusively discriminate between current sheet and solar wind effects. Analysis of the polar projected images shows that the latitudinal location of the ME is changing substantially over long periods of time. It also shows that the footprint of Ganymede follows the same trend as the ME. This latter finding puts strong constraints on the origin of the shifts. We use the VIP4 magnetic field model developed by *Connerney et al.* [1998] to suggest that internal variations of the current sheet parameters might be used as an alternative to the changing solar wind conditions to explain the latitudinal shifts of the auroral emissions. The present work does not rule out solar wind induced magnetospheric reconfiguration as a key process for shaping the auroral morphology. However, we suggest that internally driven current sheet fluctuations are able to give rise to similar effects.

2. Data Sets and Reduction

[6] We have considered 6 HST data sets obtained from 1997 to 2006 (Table 1). They consist of FUV images obtained with the STIS and ACS cameras in the Clear and filtered modes. The Clear mode is sensitive to the H_2 Lyman and Werner band emissions as well as to the strong H Ly-α line, while the filtered mode rejects most of the Ly-α photons. Where possible, we favored the filtered images because the filtering considerably reduces geocoronal contamination and gives rise to a sharper planetary limb, at the cost of somewhat lower sensitivity. The improved limb fitting thus provides a more accurate jovicentric mapping of the auroral emissions. The images are then corrected, calibrated, and projected onto polar maps, following the procedures described by *Grodent et al.* [2003a, 2005]. Owing to the strong asymmetry of Jupiter's internal planetary field, a better view of the Jovian auroral emissions is obtained from Earth orbit for the northern hemisphere than for the southern. Consequently, we concentrate on the images displaying the northern auroral region.

3. Observations

3.1. Demonstration Case

[7] A striking example of auroral location variation is illustrated in Figure 1. It shows the superposition of the polar projection of two images of the northern aurora obtained with HST (~100 s exposures) more than four years apart. The main characteristics of the viewing geometry are summarized in Table 2. The warm red color figure corresponds to an image obtained with the STIS camera in December 2000, and the cold blue figure is an image obtained with the more recent ACS camera in April 2005. We have sufficient knowledge of the performances of the two cameras to ascertain that the differences between the two projections are not instrumental artifacts. The major technical difference between the two images arises because the STIS camera was operated in 'Clear' mode, meaning that all the H_2 and H FUV photons were counted, while the

Table 1. List of the HST Datasets Considered in the Present Study

HST Program ID	Year(s)	Camera
7308	1997, 1998, 1999, 2001	STIS
8171	1999, 2000	STIS
8657	2000–2001	STIS
9685	2003	STIS
10140	2005	ACS
10507	2006	ACS

ACS image was obtained with the F125LP filter which rejects most of the H Ly-α emission. The H Ly-α contribution represents approximately 30% of the total FUV emission. It originates mostly from electron impact dissociation of H_2. According to the energy degradation model described by *Grodent et al.* [2001], the contribution from direct excitation of H, at a higher altitude owing to the larger scale height of H compared to H_2, represents approximately 1% of the total auroral Ly-α emission and can thus be neglected. This contribution depends on the energy spectrum of the impinging auroral electrons, but with realistic distributions, meeting multispectral observational constraints, the ratio remains on the same order of magnitude. As a consequence, the vast majority of Ly-α photons are produced at the same altitude as the H_2-FUV photons and do not change the auroral morphology. The sole difference could result from methane absorption of the emission below 130 nm, including the Ly-α line. However, this absorption takes place near or below the homopause and may not change the absorbed emission peak altitude by more than 100 km, which is smaller than a pixel in the images. Accordingly, the presence of H Ly-α emission in the unfiltered STIS image and not in the filtered ACS image is not a source of measurable differences between the global morphologies.

[8] The images were projected on a 10° spaced grid fixed to the planet (i.e., fixed in System III) so that the projections may be directly compared. These two images were selected for their viewing similarities: the CMLs average to 117.9°, with 1.4° difference which provides an optimal view of the northern auroral region between S3 longitudes 50° and 200°. The averaged orbital phase of Io is about 243° (dusk side) and differs by only 1.8° in the two images. The averaged orbital phase of Ganymede is about 132° (post dawn sector) and shows a somewhat larger variation of 15°. It should be noted that, in this longitude range, the field lines mapping to Ganymede are tightening toward Jupiter and a 15° longitude difference in the equatorial plane magnetically maps to a longitude difference of 6° in the Jovian ionosphere. The most pronounced difference between the two viewing geometries is the sub-Earth latitude. It changed from a positive value of 3.08°, favoring the viewing of the northern hemisphere, to a negative latitude of −2.83°. This difference shows up in Figure 1 as the extension near the planetary limb of the bluish projection, corresponding to the negative sub-Earth latitude, is smaller than that of the reddish projection. It should be emphasized that the variation of the sub-Earth latitude is fully taken into account in the polar projection procedure.

[9] At first sight, the two images roughly bear the same basic components: a main emission, polar emissions, Io footprint and its tail, and Ganymede footprint. A closer inspection reveals that the brightness distribution and location of these components drastically differs from one image to the other. The sole exception is the footprint of Io and its trailing tail which overlap almost perfectly in the dusk sector (near 90° S3) of the two projections.

3.2. Main Auroral Emission

[10] The morphology of the main emission is very different: in the STIS projection (red) the emission forms a continuous narrow ribbon around the magnetic pole from dawn to dusk. The brightness distribution along this path is far from uniform, but the continuous alignment of the emission suggests that a closed reference contour might be defined from this emission. In the ACS projection (blue), there is no such 'closed' structure. The main emission is restricted to a short arc in the morning sector (170°–200° S3) and does not permit one to draw a reference contour. There is no bright organized emission in the afternoon sector (90°–170° S3). Instead, the emission forms faint and diffuse patches roughly aligned with the 160° meridian and confined to longitudes larger than 140°. The lower latitude portion of this emission, near latitude 60°, forms a very complex structure roughly shaped like a circle. In the STIS image, the emission equatorward of the afternoon section of the main emission extends several tens of degrees away from the main emission, almost reaching the footprint of Io. The most surprising difference is the large shift between the narrow arcs in the 170°–200° morning sector. The ACS arc (blue) is up to 3° poleward of the STIS arc (red). This deviation is larger than the accuracy of the projection procedure, mainly limited by the planetary limb fitting method [*Grodent et al.*, 2003a]. Accuracy tests were specifically performed on these two images. Following *Grodent et al.* [2003a] a 4-pixel shift perpendicular to the CML was applied to the images in order to evaluate the effects of inaccurate center finding on the absolute location of auroral features, and of the different sub-Earth latitudes. It turns out that for both images, the location of Ganymede's footprint changed by only a fraction of a degree, mainly in longitude. The latitude of the main emission crossing the 180° meridian (S3) is almost unchanged because in this sector the deviation is mainly in longitude. On the other hand, the latitude change of the emission crossing the 190° meridian reaches almost 1° for the ACS image, less for the STIS image. This difference stems from the increasing mapping inaccuracy toward the planetary limb. As a consequence, the comparison between the two images was restricted to the 100°–180° S3 sector.

3.3. Ganymede Footprint

[11] Another surprising difference is the large deviation of the Ganymede footprint latitude. According to the VIP4 model, the latitude shift corresponding to the observed variation of the footprint longitude should be on the order of 0.1°. In Figure 1, the latitudinal shift is on the order of 2°, again significantly larger than the accuracy of the projection which decreases to ∼1° near the CML. This latitude shift is so large that the ACS (blue) Ganymede footprint appears at latitude larger than that of the STIS (red) main emission. Note that it does not mean that the footprint of Ganymede was poleward of the ME, since we are comparing two different projections (red – blue) obtained several years

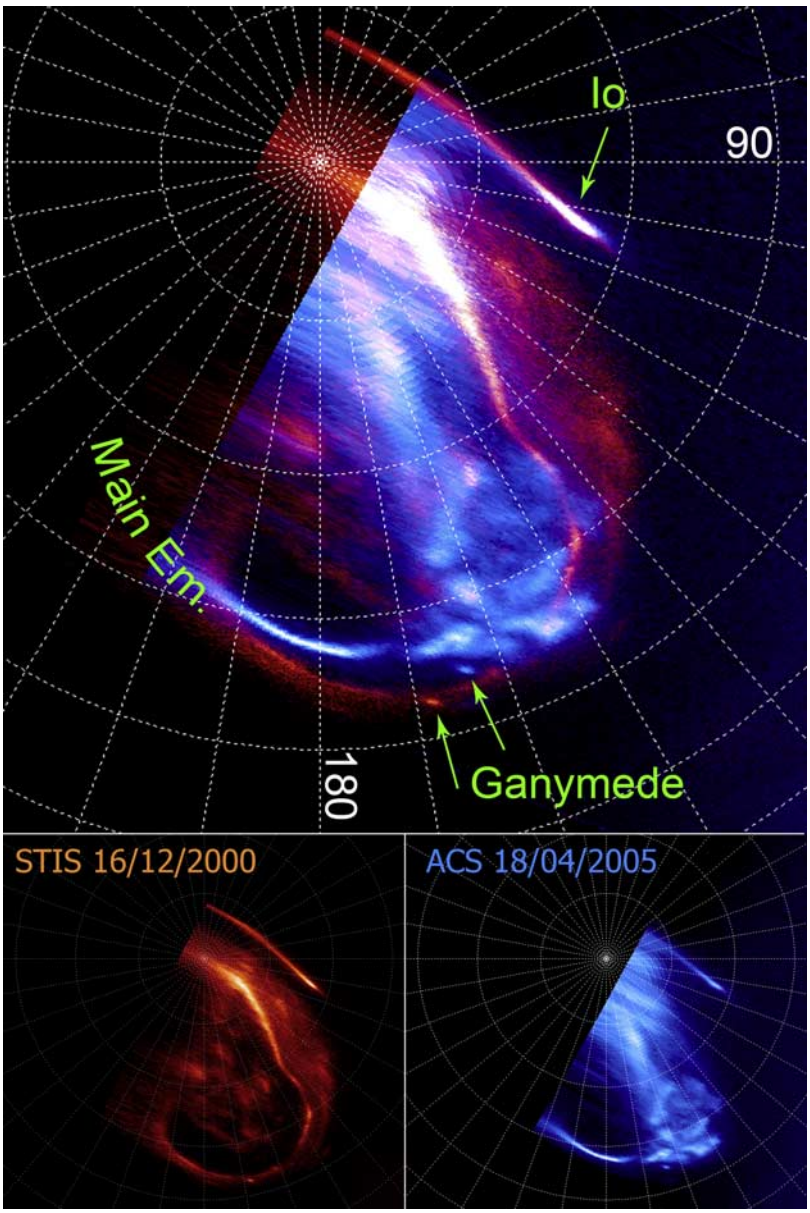

Figure 1. Top panel: Superposition of the polar projection of two images of the northern aurora obtained with HST more than four years apart. The main characteristics of the viewing geometry are summarized in Table 2. The warm red color figure corresponds to an image obtained with the STIS camera in December 2000, and the cold blue figure is an image obtained with the ACS camera in April 2005 (see bottom panels). The 90° and 180° System 3 meridians have been highlighted on a 10° spaced grid. Green arrows point to the footprints of Ganymede and Io. The main emission has also been marked in green. According to the VIP4 magnetic model, for a CML value of ~120°, at the orbit of Ganymede, Magnetic Local Time noon is along the 150° meridian. Bottom panels: Individual polar projections using the same longitude system as in top panel.

apart and the ME and the footprint of Ganymede shifted simultaneously. So far, all images showing the footprint of Ganymede, including the two projections shown in Figure 1, display it equatorward of the ME. In some of them it is very close to the ME and eventually merges with it, but always on the equatorward side.

3.4. Polar Emissions

[12] The polar emissions are also showing different features. They are usually divided into three substructures [*Grodent et al.*, 2003b]: the dark region, almost devoid of emission and located in the morning sector; the active region, characterized by strong transient brightenings and located in the post-noon sector; and the swirl region, formed by fast moving faint patches of emission near the magnetic pole. In the STIS projection (red) the dark region is well defined between the main emission and the swirl region. It extends in the afternoon region where it separates the main emission from a relatively faint active region. The morphol-

Table 2. Main Characteristics of the Viewing Geometries Relevant for the Two Images Considered in Figure 1[a]

Image ID	Date	Time	Instr.	Filter	Sub- lat.	CML	Io Phase	Gan. Phase
o6ba03uoq	16/12/2000	11:10:17	STIS	Clear	3.08°	117.2°	244.0°	124.4°
J93e03bvq	18/04/2005	11:12:40	ACS	F125LP	−2.83°	118.6°	242.2°	139.4°

[a]The central meridian longitude (CML) is given in S3, and the sub-Earth latitude is a planetocentric latitude. The orbital phase of Io and Ganymede is counted counter-clockwise, with 180° facing the observer. The F125LP filter rejects most of the Ly-α emission.

ogy is quite different in the ACS (blue) projection. The dark region is fully contained in the morning sector. The swirl region is very faint, partly 'covered' by the emission lying along the 160° meridian. The signature from the active region is not clear and, again, cannot be fully discriminated from the 160° meridian low-latitude emission.

4. Other Examples

[13] The example discussed above is rather extreme but it is not an isolated case. Figure 2 presents other cases organized in three CML ranges. The main auroral emission and the footprint of Io and its tail have been represented by curves in order to facilitate the comparison between polar projections of several images. The curves are equivalent to partial reference contours locating continuous strips of emission such as the morning arcs shown if Figure 1. The projections have the same format as in Figure 1. The main properties of each case are summarized in Table 3. The CML ranges, 115°–122° for panel A, 182°–183° for B, and 229°–232° for C, were designed to be as narrow as possible in order to compare images obtained with very similar viewing geometries, and also to put forward possible local time (LT) effects. It appears that comparable latitudinal shifts, of order of 2°, are observed in the three ranges. However, this shift can only be estimated for the narrow arc of emission which is usually forming in the pre-dawn to post-noon sector. Accordingly, it may only be ascertained that the variation of the auroral location takes place, at least, in the pre-dawn to post-noon sector. As a result of the distortion of the magnetic field lines out of the meridian plane, this LT sector is magnetically mapping to a larger region of the magnetosphere. The modified magnetic mapping is a possible cause of the latitudinal shift and will be thoroughly addressed in the discussion section.

[14] Additionally, we note that panel A of Figure 2 includes the two images appearing in Figure 1 and Table 2. They are compared with three images obtained in 1997, 2003, and 2006. Therefore this panel spans more than 7 years of observation with HST. In addition, the reference curve derived from in situ observations of the auroral emission in the visible wavelength range obtained with the Galileo spacecraft has been marked with diamonds in panel A. These short in situ exposures (several seconds) were taken on 5 and 8 November 1997 during ~1 h periods, in Jupiter's nightside. Important issues about the Galileo reference curve will be discussed elsewhere [Grodent et al., in preparation]. For the present case, it is interesting to note that the Galileo curve is best matched by the o43b09b3q yellow curve, which corresponds to the HST image taken four weeks before the Galileo images. This and the discussion of Figure 1 suggest that the auroral location variation is a long term process occurring with a timescale larger than several days rather than shorter timescale effects, such as, e.g., compressions or expansions of the magnetosphere, and/or local time effect. However, the overlap of the two curves could be fortuitous and the relatively poor sampling rate of the present database does not permit us to conclusively discriminate between short term and long term processes.

[15] Panel B of Figure 2 confirms the trend appearing in panel A with a latitudinal shift up to 3°. It consists of four images obtained in 2001, 2003, 2005, and 2006. In this tight CML range, the Io footprint is distributed over very different longitudes and does not give rise to any overlap. On the contrary, Panel C shows the comparison between two polar projected images obtained in 2001 and 2003 for which the footprint of Io and its tail are overlapping, while at the same time there is a measurable latitudinal shift, 1° to 2°, of the main emission curves.

5. Discussion and Interpretation

[16] *Hill* [2001] suggested that a 2° equatorward shift of auroral latitude at midnight compared to noon would require an outward mass-transport rate of the magnetospheric plasma which would be, plausibly, a factor-of-four larger at midnight than at noon. However, the shift of the auroral footprint location of Ganymede and of the main auroral emission is observed in images obtained with similar CMLs. Therefore the day-night magnetospheric asymmetry cannot explain the results of Figure 1.

[17] At the same time, *Hill* [2001] (equation 1) showed that the characteristic distance at which corotation breakdown becomes significant is mainly controlled by the rate of outward mass transport, and, to less extent, by the effective Pedersen conductance of Jupiter's ionosphere. It is possible that corotation breakdown occurred at a larger distance in 2005 than in 2000, in the same local time sector, as a result of an important temporal change of the iogenic plasma outward mass transport. However, a 3° shift of the auroral latitude would require a variation of the mass transport by a factor of 7 (Hill, personal communication) between 2000 and 2005, i.e., a significant change. On the other hand, it should be remembered that equation 1 from *Hill* [2001] implies a simplistic model which does not take into account the field line stretching induced by the azimuthal current flowing in the current sheet. It is most likely that whatever causes the plasma mass transport rate to change by such a large amount will also affect the current sheet and therefore the magnetic field topology near the current sheet and, in fine, the location of Ganymede's footprint. A tentative explanation is discussed below; it involves variations of the magnetic mapping from the equator to the ionosphere resulting from changes of the magnetic field line topology.

[18] According to *Connerney et al.* [1996], the absence of compelling evidence for a significant secular variation of the Jovidipole over nearly 20 years suggests that the inner

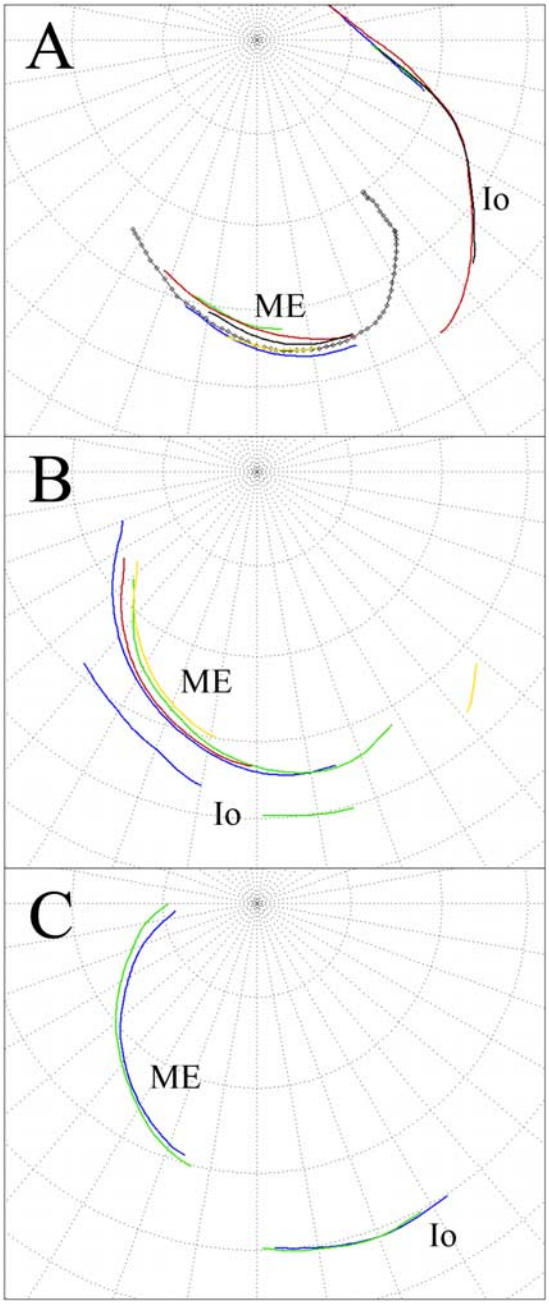

Figure 2. Other cases showing auroral latitudinal shifts organized in three CML ranges : 115°–122° for panel A, 182°–183° for B, and 229°–232° for C. The main auroral emission and the footprint of Io and its tail have been represented by curves in order to facilitate the comparison between polar projections of several images. The curves are equivalent to partial reference contours locating continuous strips of emission such as the morning arcs showing up if Figure 1. The projections have the same format as in Figure 1 (180° meridian toward the bottom, 90° to the right). The different line styles are identified in Table 3.

magnetic field is highly stable. On the contrary, *Russell et al* [2001] suggested that the dipole tilt angle has increased by 0.5° and the dipole moment has increased about 1.5% from 1975 to 2000. In any case, these secular variations are far too small to account for the dramatic deviation of the auroral emissions location and it is therefore unlikely that the internal magnetic field is the cause of the poleward shift of the emission observed in Figures 1 and 2. Nevertheless, in the inner and middle magnetosphere, the total magnetic field is the sum of an internal field and an external contribution owing to strong azimuthal currents flowing in the magnetodisc and giving rise to the current sheet. In the outer magnetosphere, mapping to higher latitudes in the ionosphere, magnetopause and cross-tail currents should also be considered.

[19] Physically, the current sheet is believed to be formed by the combined action of the centrifugal force of the quasi-corotating cool dense iogenic plasma which is transported outward from Io's vicinity, and the pressure force exerted by the hot tenuous magnetospheric plasma which is simultaneously transported inward [*Bunce and Cowley*, 2001a]. Io is a variable source of plasma. *Delamere and Bagenal* [2003] have shown that the net plasma production rate, resulting from the ionization of the neutral clouds sputtered from Io's atmosphere, ranges from 0.2 to 0.6 ton/s. In addition, they showed that these production rates are consistent with a timescale for replenishment of the torus of 19 days. The ions are thus temporarily stored in the torus for several tens of days before they are transported radially outside the torus where they populate the middle and outer magnetosphere. According to *Vasyliunas* [1983, equation 11.56], the height integrated azimuthal current density in the sheet is proportional to the plasma content of a flux tube per unit magnetic flux. It is therefore reasonable to assume that the current sheet current density value is influenced by the iogenic plasma source variations, i.e., its strength may also vary by a factor of ~3 over a period of c.a. one month, although the buffering action of the torus probably softens this variation. Modeling of the in situ magnetic field measurements obtained by Voyager 1 and 2, Pioneer 10 and Ulysses [*Connerney et al.*, 1981, 1996] have shown that the model current density may vary by up to 50% (factor 1.5) over the time period separating the different spacecraft flybys. One limitation of such modeling arises because it employs an axisymmetric current distribution tailored to fit the observations. *Khurana* [2001] and *Bunce and Cowley* [2001b] have shown that the azimuthal current strength varies as a function of local time, being strongest near midnight and systematically weakening toward the noon sector. However, we implicitly assume that the variations of the current sheet current density affect all local times proportionally.

[20] We have used the VIP4 magnetic model described by *Connerney et al.* [1998] in order to estimate the effects of a current sheet current density variation on the auroral morphology. The basic idea is that the external magnetic field associated with this current stretches the field lines away from the planet. In other words, a smaller current will have less influence and the field lines will be more dipolar. As a result, the less stretched field lines threading a given magnetic latitude in the ionosphere will cross the equatorial plane at a smaller radial distance from the planet than with the original, larger, current. Conversely, the field lines passing at a given radial distance will map to larger magnetic latitude, and the auroral morphology will be shifted poleward with a smaller current. This is illustrated

Table 3. Main Characteristics of the Images Used in Panels A, B, and C of Figure 2[a]

Image ID	Date	Time	Instr.	Filter	Sub- lat.	CML	Io Phase	Gan. Phase	Latitude	Panel	Color
o6ba03u0q	16/12/2000	11:10:17	STIS	Clear	3.08	117.2	244.0	124.4	54.7	A	blue
j93e03bvq	18/04/2005	11:12:40	ACS	F125LP	−2.83	118.6	242.2	139.4	57.8	A	green
o43b09b3q	01/12/1997	04:06:06	STIS	SrF2	0.09	115.6	293.4	113.8	55.6	A	yellow
o5hya4i4q	21/09/1999	20:27:30	STIS	SrF2	3.35	121.6	176.1	110.4	57.3	A	red
o8k801pqq	25/02/2003	23:27:49	STIS	SrF2	0.14	115.0	196.4	68.0	56.9	A	black
Galileo	5–8/11/1997	—	SSI	—	0.02	—	—	—	55.6	A	◇-◇-◇-
o6baa5bmq	21/01/2001	22:21:17	STIS	Clear	2.93	182.8	106.7	161.8	63.7	B	blue
j9du04faq	14/04/2006	04:26:18	ACS	F125LP	−3.41	182.2	169.3	255.4	65.2	B	green
j93ea3cjq	18/04/2005	12:58:11	ACS	F125LP	−2.83	182.4	257.2	143.1	65.7	B	yellow
o8k802g0q	24/02/2003	19:32:45	STIS	SrF2	0.14	182.3	319.3	9.4	64.4	B	red
o8k801qzq	26/02/2003	02:36:47	STIS	SrF2	0.15	229.2	223.2	74.6	74.5	C	blue
o6baa7y4q	20/01/2001	17:55:27	STIS	SrF2	2.93	231.6	225.5	102.2	72.9	C	green

[a]The SrF2 filter used in STIS images plays the same role as the F125LP filter applied to the ACS images. Longitude and latitude systems are the same as for Table 2. The "latitude" column gives the ME latitude in degrees at S3 longitude 180° for panel A, 210° for panel B, and 240° for panel C. The "color" column refers to the colors used in Figure 2. The first two images are the same as those considered in Figure 1 and Table 2. The Galileo reference contour was determined from several images obtained at different times. Accordingly, some time dependent parameters could not be displayed (—).

in Figure 3 where we have plotted the ionospheric footpaths of field lines mapping to different radial distances for a current density characterized by a current constant (I_0) of 25.6 MA/R_J (red dots contours) and 8.5 MA/R_J (blue crosses contours) (following the formalism used by *Connerney et al.* [1998]), corresponding to the current density ($I = I_0/\rho$, where ρ is the radial distance in R_J) determined by *Connerney et al.* [1998] to fit the Voyager 1 and Pioneer 10 observations, and a three times smaller current density, respectively. We considered the field lines mapping to the orbit of Io (5.9 R_J, equatorward contour), the orbit of Ganymede (15 R_J, middle contour) and to an assumed distance of 25 R_J (poleward contour) corresponding to the corotation breakdown region in the dayside magnetodisc and which fits the ME in Figure 1. The red and blue large dots between the 160° and 170° S3 meridians represent the footprint of Ganymede corresponding to the two viewing geometries described in Table 2 and shown in Figure 1. According to *Khurana* [2001], the azimuthal current in the inner magnetosphere derived from in situ Galileo observations is comparable with the current strength estimates given by *Connerney et al.* [1998]. At this point, it should be remembered that corotation does not break down at a fixed radial distance but it strongly varies with local time. In the nightside this distance may reach 60 R_J and one may not try to fit all the ME with a constant L-shell footpath.

[21] As expected, the closed paths derived with the smaller current are poleward of the paths derived with the original current. A closer look at Figure 3 reveals that even though this simulation is somewhat oversimplified, it is in good agreement with the observation depicted in Figure 1. The footprint associated with the orbit of Io is little affected (less than a degree) by the current sheet current density. This is consistent with the orbit of Io being inside the inner magnetosphere where the total magnetic field is primarily controlled by the Jovian internal field. At larger distances, the influence of the current sheet grows and may become dominant in the middle magnetosphere. Consequently, the poleward shift becomes substantial for the path mapping to the orbit of Ganymede. It reaches 2.4° between the positions corresponding to the orbital phases given in Table 2. The poleward shift keeps growing as one goes farther into the middle magnetosphere; for the footpath mapping to 25R_J it is about 2.8° at 170° of longitude.

[22] The variation of the current sheet strength may therefore provide an explanation for the shifts of the morning side ME observed in Figure 1 and Figure 2. Most importantly, it also gives a plausible explanation for observing the footprint of Ganymede in the ACS image of Figure 1 at a location poleward of the main emission *and*

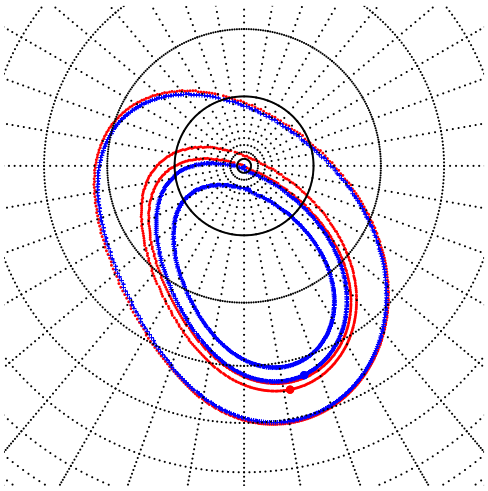

Figure 3. Ionospheric footpaths of field lines mapping to the orbit of Io (5.9 R_J), the orbit of Ganymede (15 R_J) and to an assumed distance of 25 R_J fitting the dawn to noon portion of the ME in Figure 1. The format is the same as in Figures 1 and 2. Red dots contours are calculated for a current constant (I_0, see text) of 25.6 MA/R_J corresponding to parameters selected for VIP4 (to fit the Voyager 1 and Pioneer 10 observations), and the blue "+" contours were calculated for a current constant of 8.5 MA/R_J, i.e., a three times smaller current. The large dots represent the footprint of Ganymede corresponding to the viewing geometries described in Table 2 and shown in Figure 1. While the footpath mapping to the orbit of Io is almost unchanged, the lessening of the sheet current gives rise to a significant poleward shift of the footpaths mapping to Ganymede and to 25 RJ. The blue and red colors refer to the colors used in Figure 1.

poleward of the footprint observed in the STIS image, obtained more than four years earlier with a similar observing geometry. In this particular case, it appears that varying the current density by a factor of three is sufficient to explain the poleward shift of the emission. This current density variation is twice larger than the values obtained from in situ magnetic field measurements, but it remains within a realistic range. Therefore we suggest that the case illustrated in Figure 1 may be considered as an extreme situation which was not encountered by the in situ observations. At this point of the discussion, it should be emphasized that the current sheet characteristics are also determined by the solar wind activity since it has been shown that, for example, the radial range of the current sheet on the dayside depends on the state of compression of the magnetosphere by the solar wind [e.g., *Bunce and Cowley*, 2001b].

[23] The thickness of the current sheet is estimated to be typically $\sim$2–8 R_J [e.g., *Bunce and Cowley*, 2001b] with the smaller values found at larger distance. Consequently, we have examined the possibility of obtaining the same latitudinal shifts as those illustrated in Figure 3 by decreasing the model current sheet thickness without changing the current density. It turned out that reducing the model current sheet thickness from 5 R_J to 2.5 R_J produces the expected latitudinal shifts.

[24] Similarly, a combination of moderate decrease of the thickness from 5 to 3 R_J, and of the sheet current density, actually the current constant I_0 from which densities are derived (see above), from 25.6 MA/R_J to17 MA/R_J, in agreement with the currents deduced by *Connerney et al.* [1981] for Voyager 1 and Voyager 2, respectively, also gives similar results. Finally, we note that changing the inner and outer radial boundaries of the current sheet does not substantially influence the location of the ME and Ganymede's footprint, even though the Io footprint is relatively sensitive to the distance of the inner boundary.

6. Conclusions

[25] Beyond the orbit of Io, the current density and the thickness of the current sheet have a measurable influence on the morphology of the northern auroral emission. The contribution of the current sheet to the total Jovian magnetic field may be attenuated by a weakening of the current density and/or the thickness of the current sheet. This in turn gives rise to a more dipolar (less stretched) field line configuration. As a consequence of this dipolarization, the auroral emission mapping to source regions beyond the orbit of Io is shifted poleward by up to 3°. It is evident that the reverse process will give rise to opposite effects, with an equatorward shift associated with an increased influence of the current sheet on the total magnetic field. It is important to stress that this conclusion applies to the auroral emission appearing in the pre-dawn to post-noon sector. In the other sectors, the auroral emission does not form narrow arcs but forms rather diffuse and changing unstructured configuration whose location is hard to define and thus difficult to compare from one data set to another.

[26] The main implication of the present study is that the observed latitudinal shift of the auroral emissions may be explained by processes other than variations of the solar wind conditions at Jupiter. This is because the current sheet variations primarily result from the variability of the internal (iogenic) plasma source feeding Jupiter's magnetosphere. It is important to insist on the fact that the present study does not rule out solar wind induced magnetospheric reconfiguration as a key process for shaping the auroral morphology. However, we suggest that internally driven current sheet fluctuations are able to give rise to similar effects. It is actually most likely that both internal (Iogenic production) and external (solar wind) mechanisms simultaneously influence the auroral morphology. A second implication is that the use of reference contours to locate the auroral emissions can be misleading, or give rise to substantial inaccuracies. At the same time, the latitudinal change of the auroral emission compared to average reference contour may be used as a proxy for estimating the importance of the current sheet parameters.

[27] **Acknowledgments.** This work is based on observations with the NASA/ESA Hubble Space Telescope, obtained at the Space Telescope Science Institute (STScI), which is operated by AURA, inc. for NASA under contract NAS5-26555. The authors are supported by the Belgian Fund for Scientific Research (FNRS) and by the PRODEX Program managed by the European Space Agency in collaboration with the Belgian Federal Science Policy Office. The authors are grateful to Steve Miller and an anonymous Reviewer for their valuable suggestions and comments.

[28] Wolfgang Baumjohann thanks Emma Bunce and Stephen Miller for their assistance in evaluating this paper.

References

Bunce, E. J., and S. W. H. Cowley (2001a), Divergence of the equatorial current in the dawn sector of Jupiter's magnetosphere: Analysis of Pioneer and Voyager magnetic field data, *Planet. Space Sci.*, *49*, 1089.

Bunce, E. J., and S. W. H. Cowley (2001b), Local time asymmetry of the equatorial current sheet in Jupiter's magnetosphere, *Planet. Space Sci.*, *49*, 261–274.

Clarke, J. T., et al. (1998), Hubble Space Telescope imaging of Jupiter's UV aurora during the Galileo orbiter mission, *J. Geophys. Res.*, *103*, 20,217.

Clarke, J. T., et al. (2002), Ultraviolet auroral emissions from the magnetic footprints of Io, Ganymede, and Europa on Jupiter, *Nature*, *415*, 997–1000.

Connerney, J. E. P., M. H. Acuña, and N. F. Ness (1981), Modeling the Jovian current sheet and inner magnetosphere, *J. Geophys. Res.*, *86*(A10), 8370–8384.

Connerney, J. E. P., M. H. Acuña, and N. F. Ness (1996), Octupole model of Jupiter's magnetic field from Ulysses observations, *J. Geophys. Res.*, *101*(A12), 27,453–27,458.

Connerney, J. E. P., M. H. Acuña, N. F. Ness, and T. Satoh (1998), New models of Jupiter's magnetic field constrained by the Io flux tube footprint, *J. Geophys. Res.*, *103*, 11,929.

Cowley, S. W. H., and E. J. Bunce (2001), Origin of the main auroral oval in Jupiter's coupled magnetosphere-ionosphere system, *Planet. Space Sci.*, *49*, 1067.

Cowley, S. W. H., and E. J. Bunce (2003a), Modulation of Jovian middle magnetosphere currents and auroral precipitation by solar wind-induced compressions and expansions of the magnetosphere: Initial conditions and steady state, *Planet. Space Sci.*, *51*, 31.

Cowley, S. W. H., and E. J. Bunce (2003b), Corotation-driven magnetosphere-ionosphere coupling currents in Saturn's magnetosphere and their relation to the auroras, *Ann. Geophys.*, *21*, 1691.

Cowley, S. W. H., J. D. Nichols, and D. J. Andrews (2007), Modulation of Jupiter's plasma flow, polar currents, and auroral precipitation by solar wind-induced compressions and expansions of the magnetosphere: A simple theoretical model, *Ann. Geophys.*, *25*, 1433–1463.

Delamere, P. A., and F. Bagenal (2003), Modeling variability of plasma conditions in the Io torus, *J. Geophys. Res.*, *108*(A7), 1276, doi:10.1029/2002JA009706.

Grodent, D., J. H. Waite Jr., and J.-C. Gérard (2001), A self-consistent model of the Jovian auroral thermal structure, *J. Geophys. Res.*, *106*(A7), 12,933–12,952.

Grodent, D., J. T. Clarke, J. J. H. Waite, and S. W. H. Kim (2003a), Jupiter's main auroral oval observed with HST-STIS, *J. Geophys. Res.*, *108*(A11), 1389, doi:10.1029/2003JA009921.

Grodent, D., J. T. Clarke, J. H. Waite, S. W. H. Cowley, J.-C. Gérard, and J. Kim (2003b), Jupiter's polar auroral emissions, *J. Geophys. Res.*, *108*(A10), 1366, doi:10.1029/2003JA010017.

Grodent, D., J.-C. Gérard, S. W. H. Cowley, E. J. Bunce, and J. T. Clarke (2005), Variable morphology of Saturn's southern ultraviolet aurora, *J. Geophys. Res.*, *110*, A07215, doi:10.1029/2004JA010983.

Hill, T. W. (2001), The Jovian auroral oval, *J. Geophys. Res.*, *106*(A5), 8101–8107.

Khurana, K. K. (2001), Influence of solar wind on Jupiter's magnetosphere deduced from currents in the equatorial plane, *J. Geophys. Res.*, *106*(A11), 25,999–26,016.

Nichols, J. D., E. J. Bunce, J. T. Clarke, S. W. H. Cowley, J.-C. Gérard, D. Grodent, and W. R. Pryor (2007), Response of Jupiter's UV auroras to interplanetary conditions as observed by the Hubble Space Telescope during the Cassini flyby campaign, *J. Geophys. Res.*, *112*, A02203, doi:10.1029/2006JA012005.

Russell, C. T., Z. J. Yu, K. K. Khurana, and M. G. Kivelson (2001), Magnetic field changes in the inner magnetosphere of Jupiter, *Adv. Space Res.*, *28*(6), 897–902.

Southwood, D. J., and M. G. Kivelson (2001), A new perspective concerning the influence of the solar wind on Jupiter, *J. Geophys. Res.*, *106*, 6123.

Vasyliunas, V. M. (1983), Plasma distribution and flow, in *Physics of the Jovian Magnetosphere*, edited by A. J. Dessler, p. 395, Cambridge Univ. Press, New York.

B. Bonfond, J.-C. Gérard, D. Grodent, A. Radioti, and A. Saglam, Laboratory for Planetary and Atmospheric Physics, Université de Liège, Belgium. (d.grodent@ulg.ac.be)